Target-Guided Synthesis Hot Paper

International Edition: DOI: 10.1002/anie.201502451
German Edition: DOI: 10.1002/ange.201502451

Epitope Targeting of Tertiary Protein Structure Enables Target-Guided Synthesis of a Potent In-Cell Inhibitor of Botulinum Neurotoxin**

*Blake Farrow, Michelle Wong, Jacquie Malette, Bert Lai, Kaycie M. Deyle, Samir Das, Arundhati Nag, Heather D. Agnew, and James R. Heath**

Abstract: *Botulinum neurotoxin (BoNT) serotype A is the most lethal known toxin and has an occluded structure, which prevents direct inhibition of its active site before it enters the cytosol. Target-guided synthesis by in situ click chemistry is combined with synthetic epitope targeting to exploit the tertiary structure of the BoNT protein as a landscape for assembling a competitive inhibitor. A substrate-mimicking peptide macrocycle is used as a direct inhibitor of BoNT. An epitope-targeting in situ click screen is utilized to identify a second peptide macrocycle ligand that binds to an epitope that, in the folded BoNT structure, is active-site-adjacent. A second in situ click screen identifies a molecular bridge between the two macrocycles. The resulting divalent inhibitor exhibits an in vitro inhibition constant of 165 pM against the BoNT/A catalytic chain. The inhibitor is carried into cells by the intact holotoxin, and demonstrates protection and rescue of BoNT intoxication in a human neuron model.*

Botulinum neurotoxin (BoNT) serotype A is the most lethal known toxin and is produced by some species of the bacterial genus *Clostridium*. BoNT/A is a chemodenervating zinc-dependent protease that prevents the Ca^{2+}-triggered release of acetylcholine in neuromuscular junctions by cleaving one of the three SNARE proteins required for synaptic vesicle formation and release.[1] BoNT/A intoxication proceeds with selective binding to neuronal receptors, cell entry through receptor-mediated endocytosis, endosome escape by pH-induced translocation, and, finally, cleavage of its SNAP-25 substrate in the cytosol.[2] BoNT/A comprises a receptor-binding heavy chain and a disulfide-linked catalytic light chain (LC). This disulfide bond must be intact for the toxin to poison neurons, but must be broken for the LC to act catalytically in the cytosol.[3] A subdomain (the "belt") structurally occludes the intact holotoxin active site (Scheme 1) so that drug-induced inhibition only occurs after belt release, which is promoted by the reduction of the disulfide link by the cytosolic environment.[4] The rapid sequestration of BoNT toxins into motor neurons limits current antibody-based therapies, whereas the occluded active site is "undruggable" by traditional protease inhibitors.[5] Recently membrane-penetrating small-molecule BoNT LC inhibitors have shown promise in vitro; however, their reported cytotoxicity indicates significant off-target interactions, and they have effective doses in the mid to high micromolar range.[6] BoNT is a potentially deadly bioweapon,[7] but is also a therapeutic and cosmetic agent, with an accompanying risk of accidental overdosing. Potent and effective inhibitors are needed.

The Sharpless group first reported on target-guided synthesis by in situ click chemistry.[8] They utilized the active site of an enzyme as a highly selective promoter of the 1,3-dipolar cycloaddition reaction to assemble a divalent inhibitor from two small-molecule libraries—one presenting an azide, the other an acetylene. Over the last several years, we have applied in situ click reactions to the discovery of peptides targeting a variety of proteins and post-translational modifications.[9] To build a BoNT inhibitor, we sought to further generalize the target-guided synthesis approach by exploiting the tertiary structure of the BoNT LC as a landscape for assembling a potent inhibitor (Scheme 1). We developed a macrocyclic peptide ligand (Inh-1; Supporting Information, Figure S1, S2) that is a substrate mimic for BoNT. Inh-1 binds to the active site with a binding affinity (K_D) of approximately 70 nM and a similar inhibition constant. We then employed an all-synthetic in situ click epitope-targeting approach[10] (Scheme 1) to identify a second peptide macrocycle (**L2**; Figure S3,4) that binds to a site a few angstroms away from the active site in the folded protein structure. **L2** exhibits a K_D value of 80 nM, but no inhibitory effects. Finally, we utilized an in situ click screen, promoted by the BoNT LC, to identify a linear peptide that connects the two macrocycles (Scheme 2). The final divalent ligand (Inh-2, Figure S5) inhibits the BoNT LC with an IC_{50} value of 165 ± 15 pM. Inh-2 is carried into neuronal cells by BoNT itself, and inhibits the holotoxin in live cells. This technique provides a potentially general route for the development of peripheral and

[*] B. Farrow, M. Wong, Dr. K. M. Deyle, Dr. S. Das, Dr. A. Nag, Prof. J. R. Heath
Division of Chemistry and Chemical Engineering
California Institute of Technology
1200 E. California Blvd, Pasadena, CA 91125 (USA)
E-mail: heath@caltech.edu
B. Farrow
Department of Applied Physics and Materials Science
California Institute of Technology (USA)
J. Malette, Dr. B. Lai, Dr. H. D. Agnew
Indi Molecular
6162 Bristol Parkway, Culver City, CA 90230 (USA)

[**] This work was supported by the Institute for Collaborative Biotechnologies (W911NF-09-0001) from the U.S. Army Research Office and the Defense Advanced Research Projects Agency (DARPA) through the Cooperative Agreement HR0011-11-2-0006, and the Jean Perkins Foundation. B.F. is supported by an HHMI International Student Research Fellowship. The following reagents were obtained through the NIH Biodefense and Emerging Infections Research Resources Repository, NIAID, NIH: Polyclonal anti-BoNT/A1 produced in sheep, NR-9584.

Supporting information for this article is available on the WWW under http://dx.doi.org/10.1002/anie.201502451.

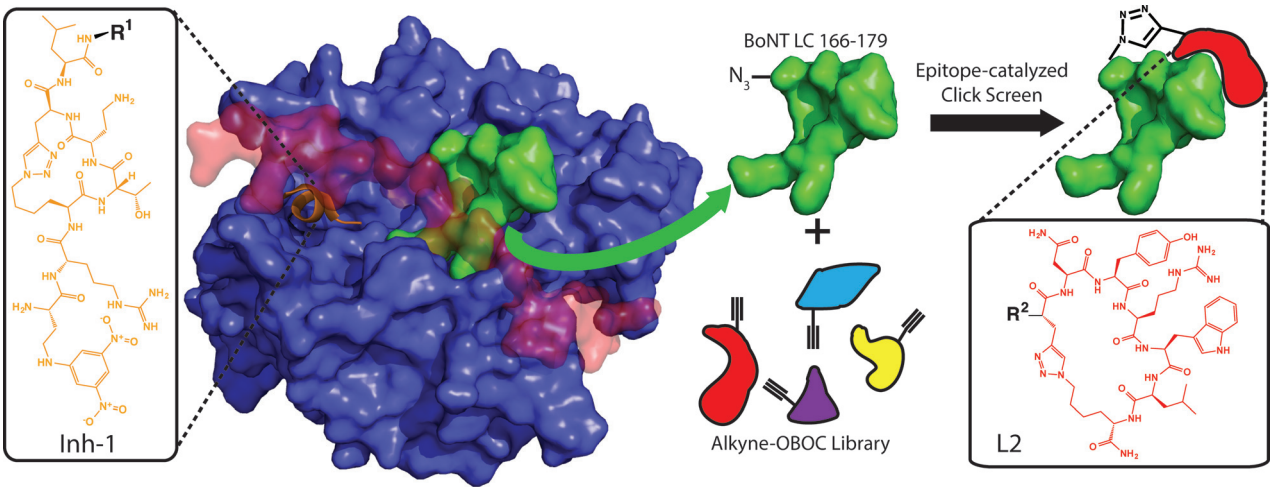

Scheme 1. The development of a biligand inhibitor of BoNT/A. Inh-1 (orange, Dab(DNP)-R-Lys(N_3)-T-Dab-Pra-L-R^1) is based on the natural peptide substrate for BoNT LC and previous structural studies of peptidomimetic substrate mimics. Epitope targeting was used to screen for a secondary ligand targeted to a nearby unstructured epitope (BoNT LC 166–179, green) exposed in the presence of the holotoxin's occluding belt (red). The ligand selected (**L2**, red, R^2-Pra-NYRWL-Lys(N_3)) was selected from a 1 100 000 member macrocyclic peptide library.

active-site binders from naïve libraries for combination through in situ click target-guided synthesis.

The active site of the catalytic BoNT/A LC recognizes the seven-residue QRATKML sequence of the SNAP-25 protein.

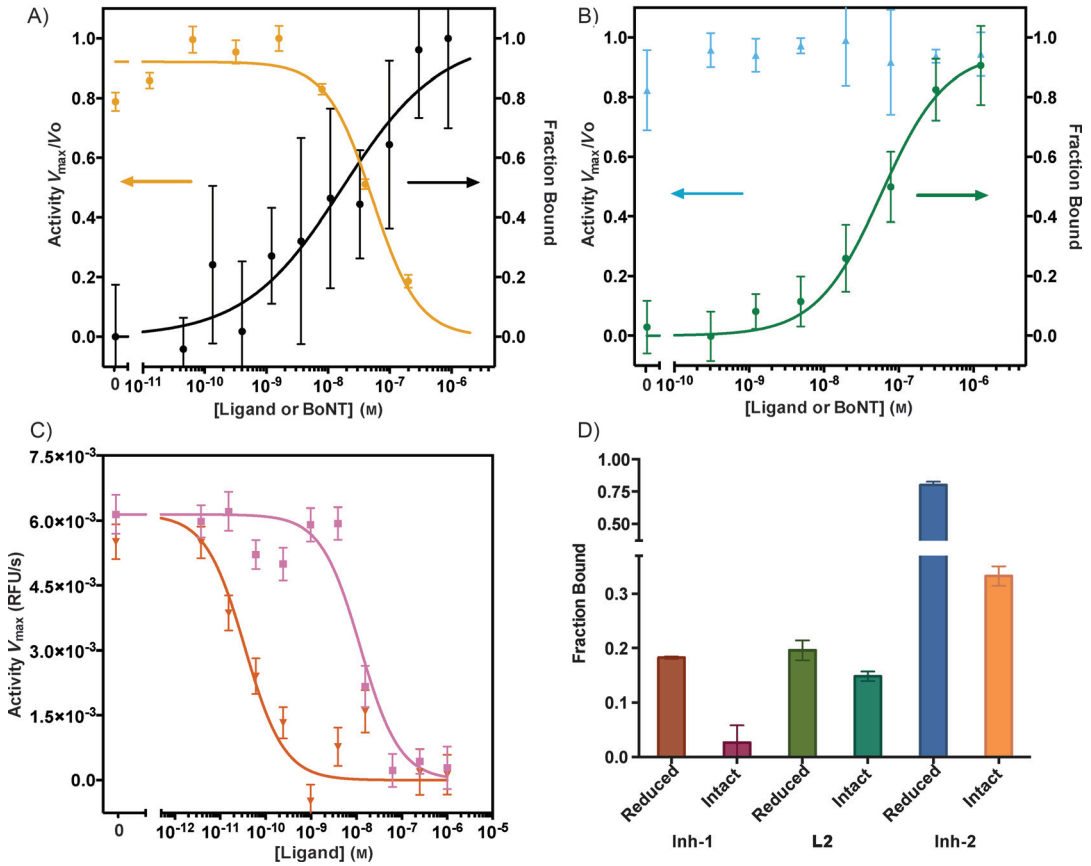

Figure 1. Characterization of ligand binding and inhibition in vitro. A) Inhibition curve (left axis) and fluorescence polarization binding curve (right axis) of Inh-1. An IC_{50} value of inhibition of 70 ± 10 nM and a K_D value of 68 ± 29 nM were obtained by Hill curve fitting. B) Inhibition curve (left axis) and fluorescence polarization binding curve (right axis) of compound **L2**. No inhibition was observed, and a K_D value of 78 ± 8 nM was determined. C) Inhibition curves comparing Inh-1 (pink) to Inh-2 (red). IC_{50} values of 60 ± 11 nM and 165 ± 15 pM, respectively, were observed. D) Single-point ELISA binding data of compounds to 50 nM of the reduced (available active site) and intact (occluded by belt) BoNT/A holotoxins. Error bars indicate standard deviation of replicates.

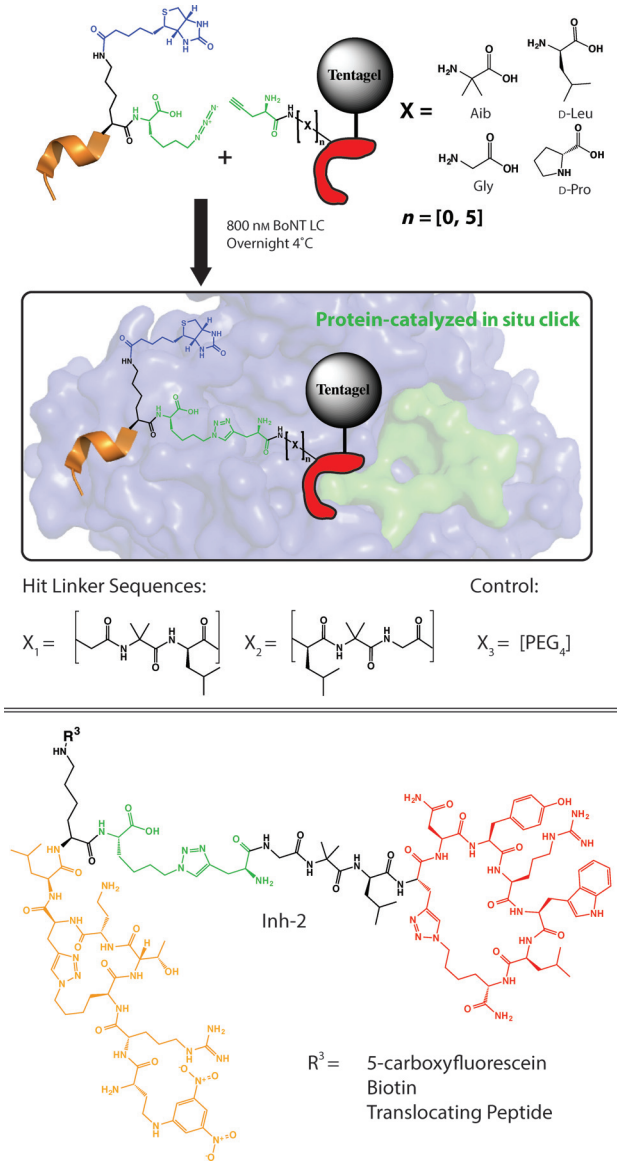

Scheme 2. Linker screen for divalent ligand development. Inh-1 was synthesized with a C-terminal azide and a biotin tag for readout of the in situ click screen and used in solution whereas **L2** was synthesized with an N-terminal alkyne and a comprehensive linker library of oligopeptides of zero to five units on Tentagel resin. An in situ protein-catalyzed click screen was performed to select for a minimally perturbative correctly oriented linker and resulted in hit sequences Gly–Aib–Leu and Leu–Aib–Gly. A PEG_4 linker was also used in preliminary assays as a comparison (Figure S13, S14). Inh-2 was the biligand chosen for all future assays.

Many inhibitors based on this motif have been reported.[5,11] One peptidomimetic inhibitor variant resulting from a structure-based search binds BoNT in a tight 3_{10} helical conformation[11b] with low nanomolar inhibition of BoNT LC in vitro (Figures S6, S7). In an effort to reinforce this conformation in solution and to increase the chemical and biological stability of this compound, we synthesized a small library of $(i,i+3)$-click-cyclized derivatives.[12]

One compound (Inh-1) inhibited BoNT/A LC with a 70 ± 8 nM inhibition constant measured in vitro using a FRET-based substrate cleavage assay (Figure S8)[13] and a K_D value of 68 ± 29 nM measured by FP and confirmed by sandwich ELISA (Figure 1A and Figure S9). However, inhibiting the full BoNT holotoxin with the occluded LC active site is more challenging. Single-point ELISA binding data (Figure 1D) shows that Inh-1 exhibits minimal binding to the holotoxin despite tight binding to the LC. Thus, we sought to expand Inh-1 to include a moiety that binds to a non-occluded region of BoNT LC adjacent to the active site. We targeted an epitope (BoNT LC residues 166–179; Figure S10) that is solvent-exposed in the occluded conformation of the holotoxin for screening with epitope-catalyzed in situ click reactions.

The epitope was synthesized with an N-terminal azidolysine and a C-terminal biotin and was screened against a 1.1M element library of macrocyclic 5-mer peptides synthesized on Tentagel resin substituted with an N-terminal propargylglycine (Scheme 2).[9f] This library was also anti-screened to remove non-specific binders to a scrambled version of the same epitope (Figures S10, S11). After incubation with the epitopes, beads were stripped, probed, and developed with an alkaline phosphatase (AP) anti-biotin mAb. Nine hit beads were sequenced using Edman degradation and found to have significant sequence homology (Figure S12). **L2** was selected after fluorescence polarization showed a K_D value of 78 ± 13 nM to the BoNT LC and similar binding (K_D not quantified) to the BoNT holotoxin, but no measurable LC inhibition (Figure 1B,D). The Inh-1 and **L2** binding sites were verified using competitive ELISA formats with known active-site binders and the targeted BoNT epitope, respectively (Figure S13).

To optimally combine Inh-1 with **L2**, kinetically controlled in situ target-guided synthesis was used with a combinatorial linker library[14] (Scheme 2) to identify an optimized molecular bridge. To this end, **L2** was synthesized on Tentagel resin and appended with an N-terminal linker library that was terminated with propargylglycine. This appended library was comprehensive from zero to five residues in four non-canonical and alternate-chirality amino acids, which were selected for structural rigidity. Our rationale was to maximize the avidity enhancement achievable when combining two independent binders by prepaying the entropic cost of orientation using a rigid linker of length equal to the root mean square average separation of the two binding sites.[15] Inh-1 was synthesized with a C-terminal azidolysine and a biotin assay handle (Figure S14). The BoNT LC was added to promote the target-guided synthesis of a bivalent ligand by bringing the reactive azide and alkyne groups in close proximity. After screening, beads were stripped, probed, and developed with an AP anti-biotin mAb. Hit beads were sequenced using Edman degradation and resulted in a consensus of two linker sequences: Gly–Aib–Leu and Leu–Aib–Gly (Scheme 2). Inh-2 was selected for all subsequent assays and demonstrated an inhibition constant of 165 ± 15 pM against BoNT LC evaluated in vitro as above. Variants of this ligand were prepared that included a biotin for binding assays, a spontaneously translocating peptide (STP) reported for the delivery of polar compounds to the cytosol, and a PEG_4 variant linker[16] (Figures S15–S17).

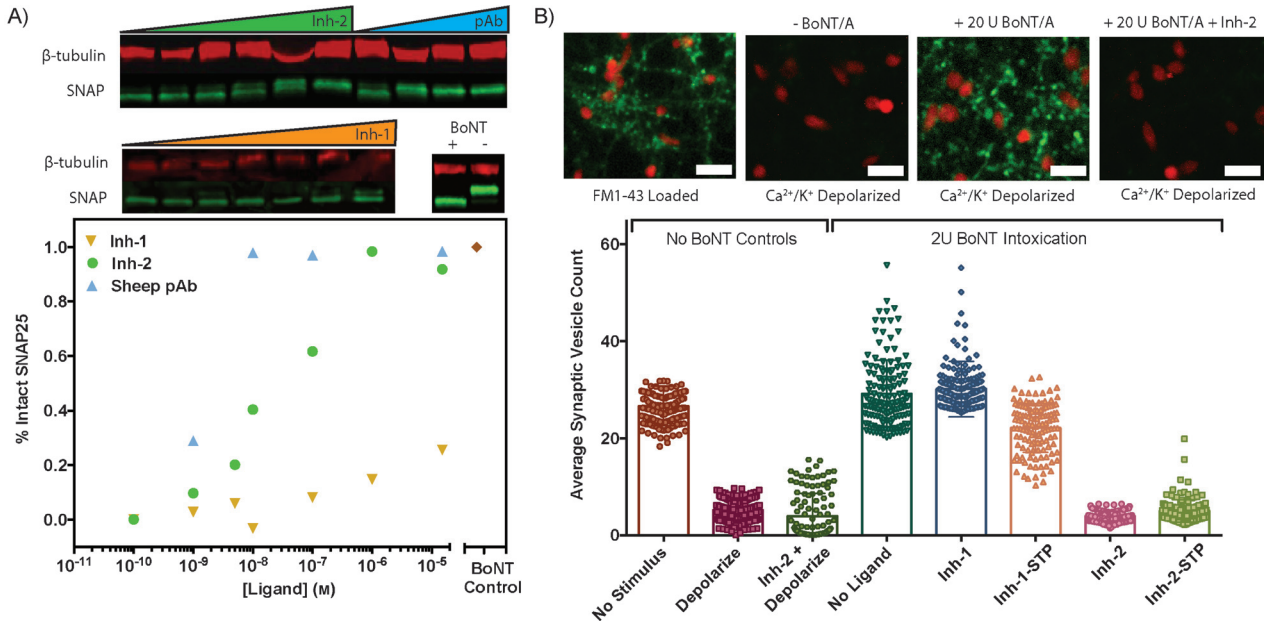

Figure 2. Ligand inhibition effect in a hiPSC-derived neuron system with BoNT holotoxin. A) Top: Western blots of neuron lysates for B-tubulin (control) and SNAP (cleaved and uncleaved). The cleaved SNAP product appears as a longer running band below the intact SNAP in the Western blot. Assays were performed with various concentrations of compounds Inh-1 and Inh-2 along with a known endocytosis-inhibiting polyclonal sheep anti-BoNT heavy-chain antibody. The plot below shows the percentage of intact SNAP as a function of ligand concentration. This percentage was calculated as the ratio of the integrated intact band intensity to the total integrated intensity of the bands. B) Top: representative epifluorescence images of live neurons after FM1-43 synaptic vesicle stain loading and after depolarization with and without prior BoNT intoxication; scale bars: 40 μm. The plot below shows the average integrated synaptic vesicle stain intensity on a per-cell basis for all conditions with 1 μM added compound where relevant. Error bars indicate standard deviation of replicates.

We tested the ability of Inh-2 to protect and rescue BoNT intoxication in human neurons (Figure 2 and Figure 3, respectively). iCell neurons are derived from pluripotent stem cells and have been reported as a model for monitoring SNAP-25 cleavage by BoNT within living cells[17] (Figure S18). Cells were plated on poly-D-lysine coated 96-well plates with a laminin matrix and exposed to two mouse LD_{50} units (U) of BoNT pre-incubated with various concentrations of Inh-1 and Inh-2. All cells were lysed after 24 hours and evaluated for SNAP-25 cleavage by Western blotting. Cleaved SNAP-25 appeared as a second band under the intact SNAP-25 band (Figure 2A). Western blotting data was quantified by densitometry to extract a dose-response behavior of the ligands in protection against BoNT intoxication. Inh-1 exhibited negligible protective effects at up to 10 μM dosing. This is likely due to the occluded active site being unavailable for binding until BoNT enters the cytosol and the membrane-impermeable nature of Inh-1. Inh-2 is also impermeable to cell membranes, but demonstrated a significant protective effect to BoNT intoxication at concentrations as low as 100 nM. This type of protection has been reported for inhibitors of the BoNT LC active site in neuron models, but only at inhibitor concentrations in the mid micromolar range.[5] As a comparison, a sheep antibody acquired from the BEI biodefense repository with a known neutralizing effect was evaluated. This antibody protects against BoNT intoxication by interrupting heavy chain receptor mediated endocytosis and provides protection into the low to mid nanomolar range.

After extended maturation, iCell neurons demonstrate functional synaptic vesicle recycling, indicating the development of a presynaptic compartment. Synaptic vesicle recycling was monitored through synaptic vesicle staining with the outer membrane partitioning styryl dye FM1-43 followed by Ca^{2+}/K^{+}-dependent depolarization[18] (Figure S19). The synaptic vesicles of BoNT-intoxicated neurons can be stained, but Ca^{2+}/K^{+} depolarization does not induce vesicle exocytosis[19] and subsequent turn-off of FM1-43 fluorescence. Synaptic vesicles appearing as puncta in epifluorescent images of the live neurons were quantified on a per cell basis (Figure S20) after exposure to BoNT pre-incubated with 1 μM of inhibitory ligands. Representative cells following depolarization are shown in Figure 2B along with the synaptic vesicle counts for each condition quantified over three wells. As observed in the Western blot assay, this functional assay shows negligible protection to BoNT intoxication by Inh-1, whereas Inh-2 provides full protection. These results are consistent with a Trojan-horse-like inhibition mechanism in which the non-inhibiting **L2** moiety of Inh-2 binds to the BoNT holotoxin, so that Inh-2 is shuttled into the cell by the holotoxin itself during the endocytosis step of BoNT intoxication. Once the belt is released, the Inh-1 moiety clamps down onto the active site, thus inhibiting the protein. To evaluate the effect of passive delivery to the cytosol, ligands were appended with an STP (Figure S21). The Inh-1–STP compound targeting the active site showed a statistically significant increase in protection ($p < 0.001$) compared to the membrane-impermeable Inh-1, but not the complete

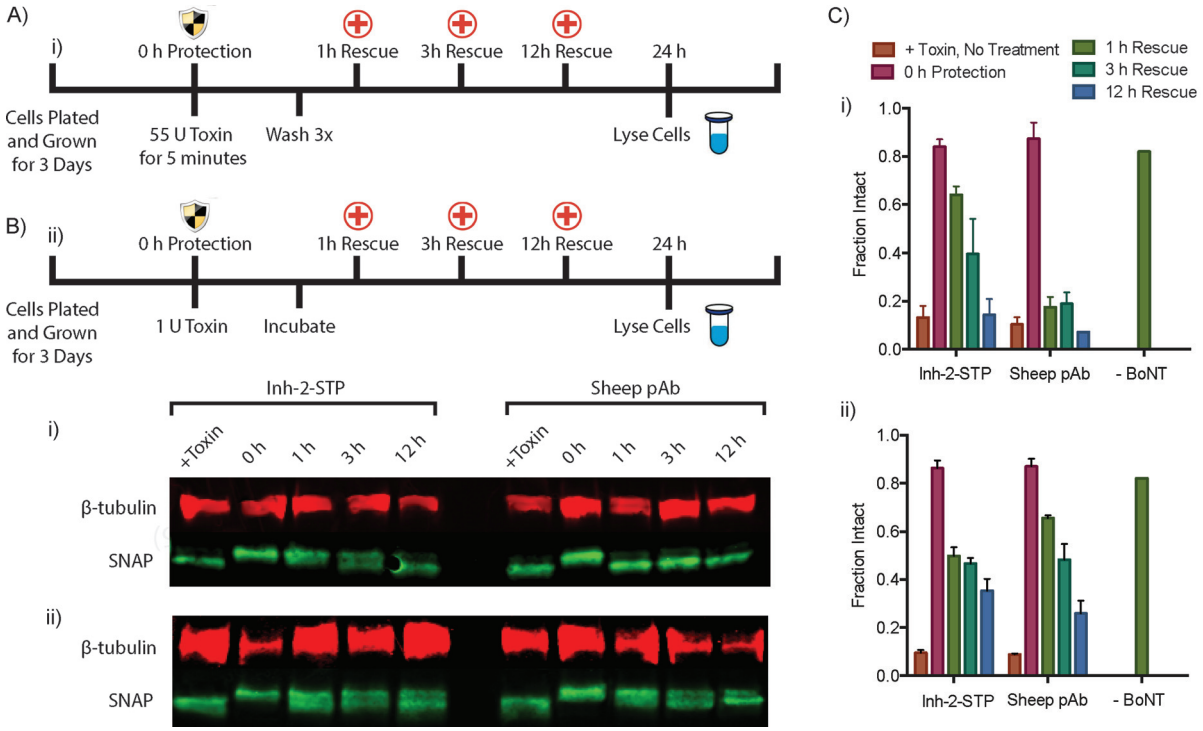

Figure 3. Rescuing hiPSC-derived neurons from BoNT intoxication. A) Experimental timeline of 55 U bolus toxin exposure (i) and 24 hour incubation with 2 U toxin (ii). The protection effect was evaluated by pre-incubation of the toxin with 1 μM inhibiting anti-BoNT pAb or Inh-2–STP, and the rescue effect was evaluated 1, 3, and 12 hours after exposure to toxin by lysing cells and quantitating SNAP cleavage by Western blot analysis and densitometry. In all cases, the cells were lysed 24 hours after toxin exposure. B) Representative Western blots of neuron lysates for B-tubulin (control) and SNAP (cleaved and uncleaved) after the rescue experiments shown in A. The cleaved SNAP product appears as a longer running band below the intact SNAP in the Western blot. C) Percentage of intact SNAP as a function of exposure time before treatment. The percentage was calculated as the ratio of the integrated intact band intensity to the total integrated intensity of the bands. Error bars indicate standard deviation of replicates.

protection expected at this concentration for the BoNT LC in vitro.

Both the membrane-permeable and -impermeable Inh-2 variants provided complete functional protection in neurons. We next evaluated the BoNT-independent cellular entry of Inh-2–STP through rescue assays in which BoNT entry and intoxication begin before the addition of the inhibitor. Rescue was evaluated in iCell neurons in a bolus 55U five-minute exposure in cell-stimulating media followed by washing and an extended 1U exposure with no washing. In both experiments, 1 μM inhibitory ligand was added to the cells 1, 3, and 12 hours post-exposure. All cells were lysed 24 hours after exposure, and SNAP-25 cleavage was evaluated by Western blotting (Figure 3B). Two blots per condition were quantified and averaged by densitometry (Figure 3C). In the bolus exposure, Inh-2–STP exhibits partial rescue from internalized BoNT as late as three hours after exposure, with later time points indicating that the internalized BoNT had completely cleaved SNAP-25 after twelve hours. This rescue effect is not observed with the Inh-2 compound lacking the STP (Figure S22). As expected, the sheep pAb showed no detectable rescue owing to its extracellular mechanism of action. In the 1U extended exposure, both the sheep pAb and Inh-2–STP showed similar levels of rescue. The process of BoNT endocytosis is slowed significantly at low concentrations and in non-stimulating media, enabling protection through the pAb protection mechanism. The rescue effect of Inh-2–STP in the absence of extracellular BoNT indicates that the STP allowed passive translocation of Inh-2 across the cell membrane for inhibition of previously internalized BoNT.

We have reported the rational use of the tertiary structure of a protein target as a landscape for the assembly of a highly potent inhibitor. The specific application yielded a ligand, Inh-2, that is a strong inhibitor in spite of the naturally occluded active site of BoNT holotoxin. Inh-2 effectively acts as a Trojan horse; it is carried into the neuronal cells by the BoNT machinery. Once inside the cytosol, the BoNT LC active site is exposed, and Inh-2 performs its inhibitory function. To the best of our knowledge, this divalent inhibitory ligand is the most potent in vitro and in cell inhibitor of BoNT/A reported to date and represents the first use of a peripheral binding site to enhance the binding avidity and facilitate BoNT/A holotoxin binding. This basic approach of identifying and combining peripheral binders may have general applicability for developing high-affinity, high-specificity enzyme inhibitors.

Keywords: botulinum neurotoxin · combinatorial screening · epitope targeting · peptides · target-guided synthesis

How to cite: *Angew. Chem. Int. Ed.* **2015**, *54*, 7114–7119
Angew. Chem. **2015**, *127*, 7220–7225

[1] a) J. Blasi, E. R. Chapman, E. Link, T. Binz, S. Yamasaki, P. Decamilli, T. C. Sudhof, H. Niemann, R. Jahn, *Nature* **1993**, *365*, 160; b) J. Blasi, E. R. Chapman, S. Yamasaki, T. Binz, H. Niemann, R. Jahn, *EMBO J.* **1993**, *12*, 4821; c) G. Schiavo, F. Benfenati, B. Poulain, O. Rossetto, P. P. Delaureto, B. R. Dasgupta, C. Montecucco, *Nature* **1992**, *359*, 832; d) G. Schiavo, O. Rossetto, A. Santucci, B. R. Dasgupta, C. Montecucco, *J. Biol. Chem.* **1992**, *267*, 23479.

[2] L. L. Simpson, *Annu. Rev. Pharmacol. Toxicol.* **2004**, *44*, 167.

[3] G. Schiavo, E. Papini, G. Genna, C. Montecucco, *Infect. Immun.* **1990**, *58*, 4136.

[4] D. B. Lacy, W. Tepp, A. C. Cohen, B. R. DasGupta, R. C. Stevens, *Nat. Struct. Biol.* **1998**, *5*, 898.

[5] C. Anne, S. Turcaud, A. G. S. Blommaert, F. Darchen, E. A. Johnson, B. R. Roques, *ChemBioChem* **2005**, *6*, 1375.

[6] a) L. M. Eubanks, M. S. Hixon, W. Jin, S. Hong, C. M. Clancy, W. H. Tepp, M. R. Baldwin, C. J. Malizio, M. C. Goodnough, J. T. Barbieri, E. A. Johnson, D. L. Boger, T. J. Dickerson, K. D. Janda, *Proc. Natl. Acad. Sci. USA* **2007**, *104*, 2602; b) P. Čapek, Y. Zhang, D. J. Barlow, K. L. Houseknecht, G. R. Smith, T. J. Dickerson, *ACS Chem. Neurosci.* **2011**, *2*, 288; c) G. E. Boldt, J. P. Kennedy, K. D. Janda, *Org. Lett.* **2006**, *8*, 1729; d) J. C. Burnett, G. Ruthel, C. M. Stegmann, R. G. Panchal, T. L. Nguyen, A. R. Hermone, R. G. Stafford, D. J. Lane, T. A. Kenny, C. F. McGrath, P. Wipf, A. M. Stahl, J. J. Schmidt, R. Gussio, A. T. Brunger, S. Bavari, *J. Biol. Chem.* **2007**, *282*, 5004–5014.

[7] a) J. C. Burnett, E. A. Henchal, A. L. Schmaljohn, S. Bavari, *Nat. Rev. Drug Discovery* **2005**, *4*, 281; b) S. C. Clarke, *Br. J. Biomed. Sci.* **2005**, *62*, 40; c) USAMRIID, *Medical Management of Biological Casualties Handbook*, 7th ed., U.S. Government Printing Office, 2011.

[8] W. G. Lewis, L. G. Green, F. Grynszpan, Z. Radic, P. R. Carlier, P. Taylor, M. G. Finn, K. B. Sharpless, *Angew. Chem. Int. Ed.* **2002**, *41*, 1053; *Angew. Chem.* **2002**, *114*, 1095.

[9] a) J. A. Pfeilsticker, A. Umeda, B. Farrow, C. L. Hsueh, K. M. Deyle, J. T. Kim, B. T. Lai, J. R. Heath, *Plos One* **2013**, *8*, e76224; b) M. Coppock, B. Farrow, A. S. Finch, B. Lai, J. Maciel, J. Heath, D. N. Stratis-Cullum, *Biopolymers* **2013**, *100*, 289; c) B. Farrow, S. A. Hong, E. C. Romero, B. Lai, M. B. Coppock, K. M. Deyle, A. S. Finch, D. N. Stratis-Cullum, H. D. Agnew, S. Yang, J. R. Heath, *ACS Nano* **2013**, *7*, 9452; d) A. Nag, S. Das, M. B. Yu, K. M. Deyle, S. W. Millward, J. R. Heath, *Angew. Chem. Int. Ed.* **2013**, *52*, 13975; *Angew. Chem.* **2013**, *125*, 14225; e) S. W. Millward, R. K. Henning, G. A. Kwong, S. Pitram, H. D. Agnew, K. M. Deyle, A. Nag, J. Hein, S. S. Lee, J. Lim, J. A. Pfeilsticker, K. B. Sharpless, J. R. Heath, *J. Am. Chem. Soc.* **2011**, *133*, 18280; f) J. R. Heath, R. D. Rohde, A. Nag, S. Das, A. Umeda, US 2015/0078999 A1, **2015**.

[10] K. M. Deyle, B. Farrow, Y. Hee, J. Work, M. Wong, B. Lai, A. Umeda, S. Millward, A. Nag, S. Das, J. R. Heath, *Nat. Chem.* **2015**, DOI: 10.1038/nchem.2223.

[11] a) J. E. Zuniga, J. T. Hammill, O. Drory, J. E. Nuss, J. C. Burnett, R. Gussio, P. Wipf, S. Bavari, A. T. Brunger, *Plos One* **2010**, *5*, e11378; b) J. E. Zuniga, J. J. Schmidt, T. Fenn, J. C. Burnett, D. Arac, R. Gussio, R. G. Stafford, S. S. Badie, S. Bavari, A. T. Brunger, *Structure* **2008**, *16*, 1588.

[12] O. Jacobsen, H. Maekawa, N. H. Ge, C. H. Gorbitz, P. Rongved, O. P. Ottersen, M. Amiry-Moghaddam, J. Klaveness, *J. Org. Chem.* **2011**, *76*, 1228.

[13] D. Caglic, K. M. Bompiani, M. C. Krutein, P. Capek, T. J. Dickerson, *J. Vis. Exp.* **2013**, *82*, e50908.

[14] X. D. Hu, R. Manetsch, *Chem. Soc. Rev.* **2010**, *39*, 1316.

[15] D. J. Diestler, E. W. Knapp, *Phys. Rev. Lett.* **2008**, *100*, 178101.

[16] J. R. Marks, J. Placone, K. Hristova, W. C. Wimley, *J. Am. Chem. Soc.* **2011**, *133*, 8995.

[17] R. C. M. Whitemarsh, M. J. Strathman, L. G. Chase, C. Stankewicz, W. H. Tepp, E. A. Johnson, S. Pellett, *Toxicol. Sci.* **2012**, *126*, 426.

[18] M. Niedringhaus, R. Dumitru, A. M. Mabb, Y. Wang, B. D. Philpot, N. L. Allbritton, A. M. Taylor, *Sci. Rep.* **2015**, *5*, 8353.

[19] E. A. Neale, L. M. Bowers, V. Dunlap, L. C. Williamson, *Mol. Biol. Cell* **1995**, *6*, 1899.

Received: March 16, 2015
Revised: April 9, 2015
Published online: April 29, 2015

